Magnetized Neutron Stars in an Interstellar Medium

Olga Toropina

Space Research Institute, Moscow

Marina Romanova and Richard Lovelace

Cornel University, Ithaca, NY

I. Introduction

Evolution of Magnetized Neutron Stars

Ejector stage - a rapidly rotating (P<1s) magnetized neutron star is active as a radiopulsar. The NS spins down owing to the wind of magnetic field and relativistic particles from the region of the light cylinder:

$$R_A > R_L$$

Propeller stage - after the NS spins-down sufficiently, the relativistic wind is then suppressed by the inflowing matter, the centrifugal force prevents accretion, NS rejects an incoming matter:

$$R_C < R_A < R_L$$

Accretor - NS rotates slowly, matter can accrete onto star surface:

$$R_A < R_C,\ R_A < R_L$$

Georotator - NS moves fast through the interstellar medium:

$$R_A > R_{acc}$$

SN NS

I. Introduction

Evolution of Magnetized Neutron Stars

Alfven radius (magnetospheric radius):

$$\rho V^2/2 = B^2/8\pi$$

for B=10^{12} G, V=100 km/c, n=1 см$^{-3}$ $\mathbf{R_A} \sim 2 \times 10^{11}$ cm

Accretion radius:

$$R_{acc} = 2GM_* / (c_s^2 + v^2) \sim 3.8 \times 10^{12} \ M/v_{100} \text{ cm}$$

Corotation radius:

$$R_C = (GM/\Omega^2)^{1/3} \sim 7 \times 10^8 \ P_{10}^{2/3} \text{ cm}$$

Light cylinder radius:

$$R_L = cP/2\pi \sim 5 \times 10^9 \ P \text{ cm}$$

I. Introduction

Accretion onto Slow Moving Star

- Classical analytical solution for non-magnetized star, Bondi (1952)

$$\frac{c_s^2}{2} = \frac{GM_*}{r}$$

$$R_B = \frac{2GM_*}{c_s^2}$$

$$M_* = 1.4\ M_\odot$$

$$c_s = 10\ \mathrm{km/s}$$

$$R_B = 2 \times 10^{14} \left(\frac{M_*}{M_\odot}\right)\left(\frac{10\frac{\mathrm{km}}{\mathrm{s}}}{c_s}\right)^2 \mathrm{cm}$$

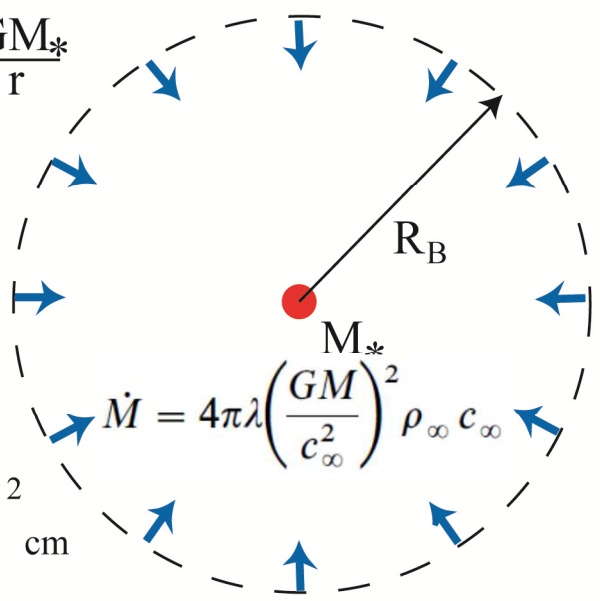

I. Introduction

Accretion onto Fast Moving Star

- Analytical solution for moving non-magnetized star - Hoyle & Lyttleton (1944), Bondi (1952)

$$\frac{v^2}{2} = \frac{GM_*}{r}$$

$$R_{acc} = \frac{2GM_*}{v^2}$$

Taking into account pressure:

$$R_{acc} = \frac{2GM_*}{v^2 + c_s^2}$$

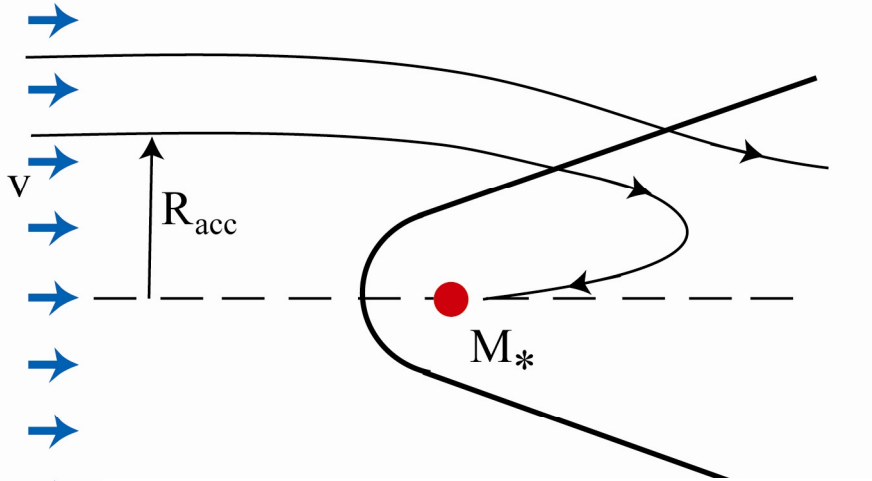

$$\dot{M}_{BHL} = \frac{4\pi\alpha(GM_*)^2\rho}{(v^2 + c_s^2)^{3/2}} \approx 7.4 \times 10^8 \frac{n}{v_{100}^3} M^2 \ \frac{g}{s} .$$

A non-magnetized star moving through the ISM captures matter gravitationally from the accretion or Bondi-Hoyle radius. And we can estimate an mass accretion rate.

I. Introduction

Luminosity of IONS

$$\dot{M}_{\rm BHL} = \frac{4\pi\alpha (G M_*)^2 \rho}{(v^2 + c_s^2)^{3/2}} \approx 7.4 \times 10^8 \frac{n}{v_{100}^3} M^2 \ \frac{\rm g}{\rm s} \ .$$

$$L = \frac{v_{ff}^2}{2} \dot{M} \approx 2.4 \times 10^{29} \frac{n}{v_{100}^3} \ \frac{\rm erg}{s}$$

- Strong dependence on velocity ~ v^{-3}
- Proportional to the density of the ISM ~ n
- Accretion rate depends on magnetic field and rotation

I. Introduction

The Influence of the Magnetic Field

- The magnetic field of the star complicates the problem, since the magnetosphere interacts with ISM

The two main cases:

1) If $R_A < R_{acc}$ a gravitational focusing is important, matter accumulates around the star and interacts with magnetic field (accretor regime)

2) If $R_A > R_{acc}$ matter from the ISM interacts directly with the star's magnetosphere, a gravitational focusing is not important (georotator regime)

A ratio between R_A and R_{acc} depends on B_* and V_* (or $\dot{M}$)

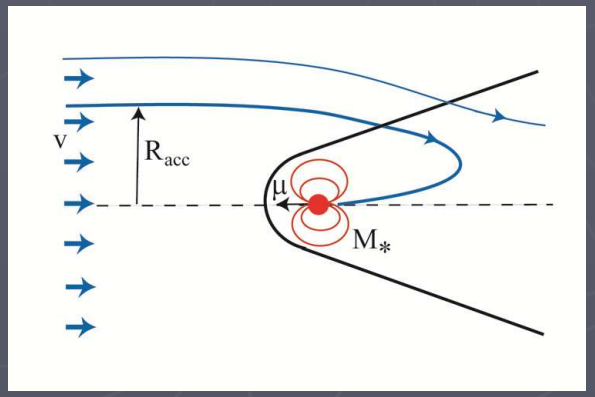

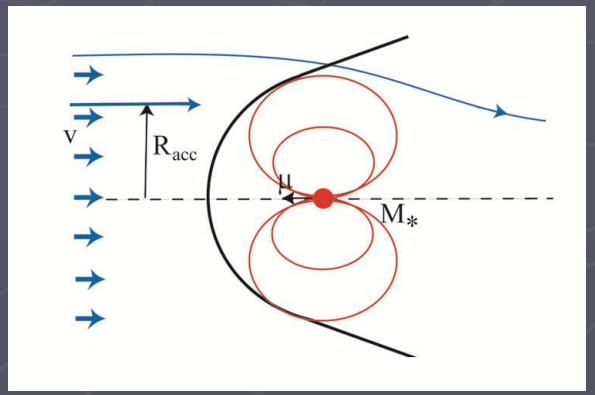

I. Introduction

Possible Geometry

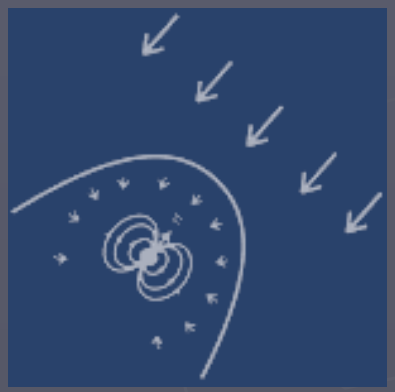

Slow NS, V<10 km/s, slow rotation, accretion

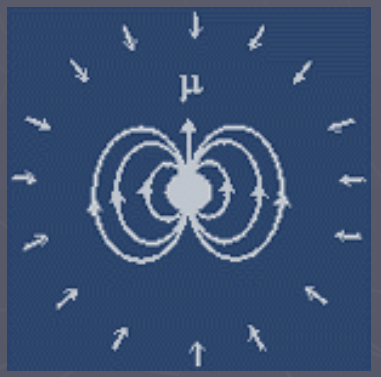

Fast NS, V> 30-100 km/s, relatively weak magnetic field, B < 10^{12} G

Fast NS, V> 30-100 km/s, strong magnetic field, B > 10^{12} G

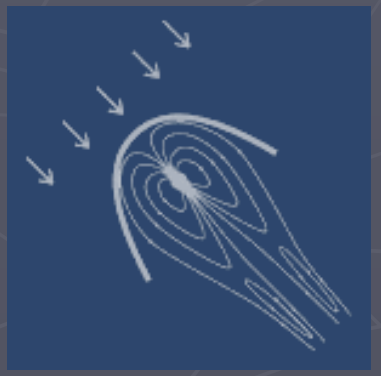

NS on the propeller stage, high Ω

II. MHD Simulation of Accretion

We consider an equation system for resistive MHD (Landau, Lifshitz 1960):

$$\frac{\partial \rho}{\partial t} + \nabla \cdot (\rho\ \mathbf{v}) = 0$$

$$\rho \left(\frac{\partial}{\partial t} + (\mathbf{v} \cdot \nabla) \right) \mathbf{v} = -\nabla p + \frac{1}{c} \mathbf{J} \times \mathbf{B} + \mathbf{F}^g$$

$$\frac{\partial \mathbf{B}}{\partial t} = \nabla \times (\mathbf{v} \times \mathbf{B}) + \frac{c^2}{4\pi\sigma} \nabla^2 \mathbf{B}$$

$$\frac{\partial (\rho\varepsilon)}{\partial t} + \nabla \cdot (\rho\varepsilon \mathbf{v}) = -p\,(\nabla \cdot \mathbf{v}) + \frac{1}{\sigma} \mathbf{J}^2$$

- $p = (\gamma - 1)\,\rho\varepsilon,\ \gamma = 5/3$
- Ohm's law $\mathbf{J} = \sigma(\mathbf{E} + \mathbf{v} \times \mathbf{B}/c)$

We use non-relativistic, axisymmetric resistive MHD code. The code incorporates the methods of local iterations and flux-corrected transport. This code was developed by Zhukov, Zabrodin, & Feodoritova (Keldysh Applied Mathematic Inst.)

- The equation of state is for an ideal gas, where $\gamma = 5/3$ is the specific heat ratio and ε is the specific internal energy of the gas.
- The equations incorporate Ohm's law, where σ is an electric conductivity.

II. MHD Simulation of Accretion

We consider an equation system for resistive MHD (Landau, Lifshitz 1960):

$$\frac{\partial \rho}{\partial t} + \nabla \cdot (\rho\, \mathbf{v}) = 0$$

$$\rho \left(\frac{\partial}{\partial t} + (\mathbf{v} \cdot \nabla) \right) \mathbf{v} = -\nabla p + \frac{1}{c} \mathbf{J} \times \mathbf{B} + \mathbf{F}^g$$

$$\frac{\partial \mathbf{B}}{\partial t} = \nabla \times (\mathbf{v} \times \mathbf{B}) + \frac{c^2}{4\pi\sigma} \nabla^2 \mathbf{B}$$

$$\frac{\partial (\rho\varepsilon)}{\partial t} + \nabla \cdot (\rho\varepsilon \mathbf{v}) = -p\, (\nabla \cdot \mathbf{v}) + \frac{1}{\sigma} \mathbf{J}^2$$

- $p = (\gamma - 1)\, \rho\varepsilon,\ \gamma = 5/3$
- Ohm's law $\mathbf{J} = \sigma(\mathbf{E} + \mathbf{v} \times \mathbf{B}/c)$

We assume axisymmetry ($\partial/\partial\phi = 0$), but calculate all three components of **v** and **B**. We use a vector potential **A** so that the magnetic field **B** = ∇ x **A** automatically satisfies $\nabla \bullet \mathbf{B} = 0$.

We use a cylindrical, inertial coordinate system (r, ϕ, z) with the z-axis parallel to the star's dipole moment μ and rotation axis Ω.

A magnetic field of the star is taken to be an aligned dipole, with vector potential

A = μ x **R**/*R*3

II. MHD Simulation of Accretion

We consider an equation system for resistive MHD (Landau, Lifshitz 1960):

$$\frac{\partial \rho}{\partial t} + \nabla\cdot(\rho\ \mathbf{v}) = 0$$

$$\rho\left(\frac{\partial}{\partial t} + (\mathbf{v}\cdot\nabla)\right)\mathbf{v} = -\nabla p + \frac{1}{c}\mathbf{J}\times\mathbf{B} + \mathbf{F}^g$$

$$\frac{\partial \mathbf{B}}{\partial t} = \nabla\times(\mathbf{v}\times\mathbf{B}) + \frac{c^2}{4\pi\sigma}\nabla^2\mathbf{B}$$

$$\frac{\partial(\rho\varepsilon)}{\partial t} + \nabla\cdot(\rho\varepsilon\mathbf{v}) = -p\,(\nabla\cdot\mathbf{v}) + \frac{1}{\sigma}\mathbf{J}^2$$

- $p = (\gamma - 1)\,\rho\varepsilon,\ \gamma = 5/3$
- Ohm's law $\mathbf{J} = \sigma(\mathbf{E} + \mathbf{v}\times\mathbf{B}/c)$

After reduction to dimensionless form, the MHD equations involve the dimensionless parameters:

$$\beta \equiv \frac{8\pi p_0}{B_0^2}\ , \qquad \tilde{\eta}_\mathrm{m} \equiv \frac{\eta_\mathrm{m}}{R_\mathrm{B} v_0} = \frac{1}{Re_\mathrm{m}}\ ,$$

$$\eta_\mathrm{m} \equiv c^2/(4\pi\sigma)$$

II. MHD Simulation of Accretion

Geometry of Simulation Region

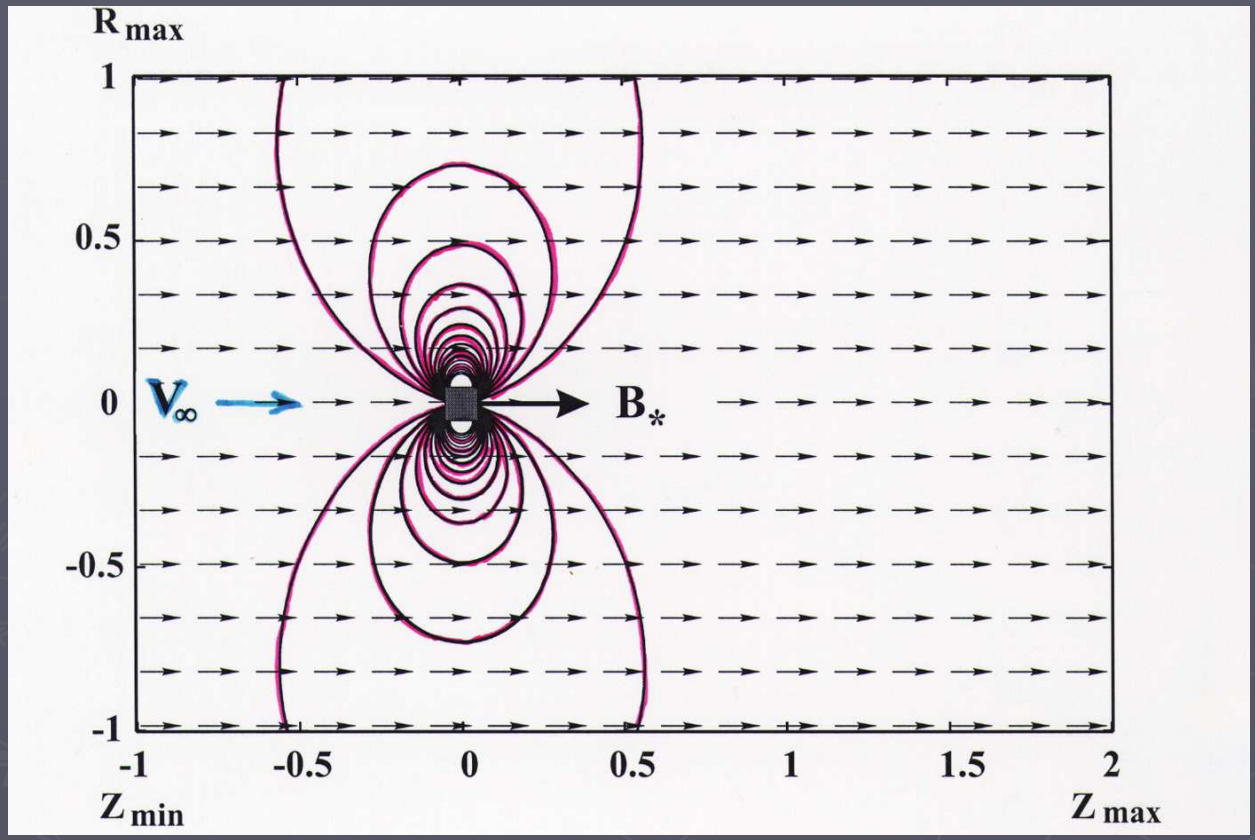

Cylindrical inertial coordinate system (r, ϕ, z), with origin at the star's center. Z-axis is parallel to the velocity v∞ and magnetic moment μ. Supersonic inflow with Mach number M from right boundary. The incoming matter is assumed to be unmagnetized. Magnetic field of the star is dipole. Bondi radius (R_B)=1. Uniform greed (r, z) 1297 x 433

II. MHD Simulation of Accretion

Hydrodynamic case

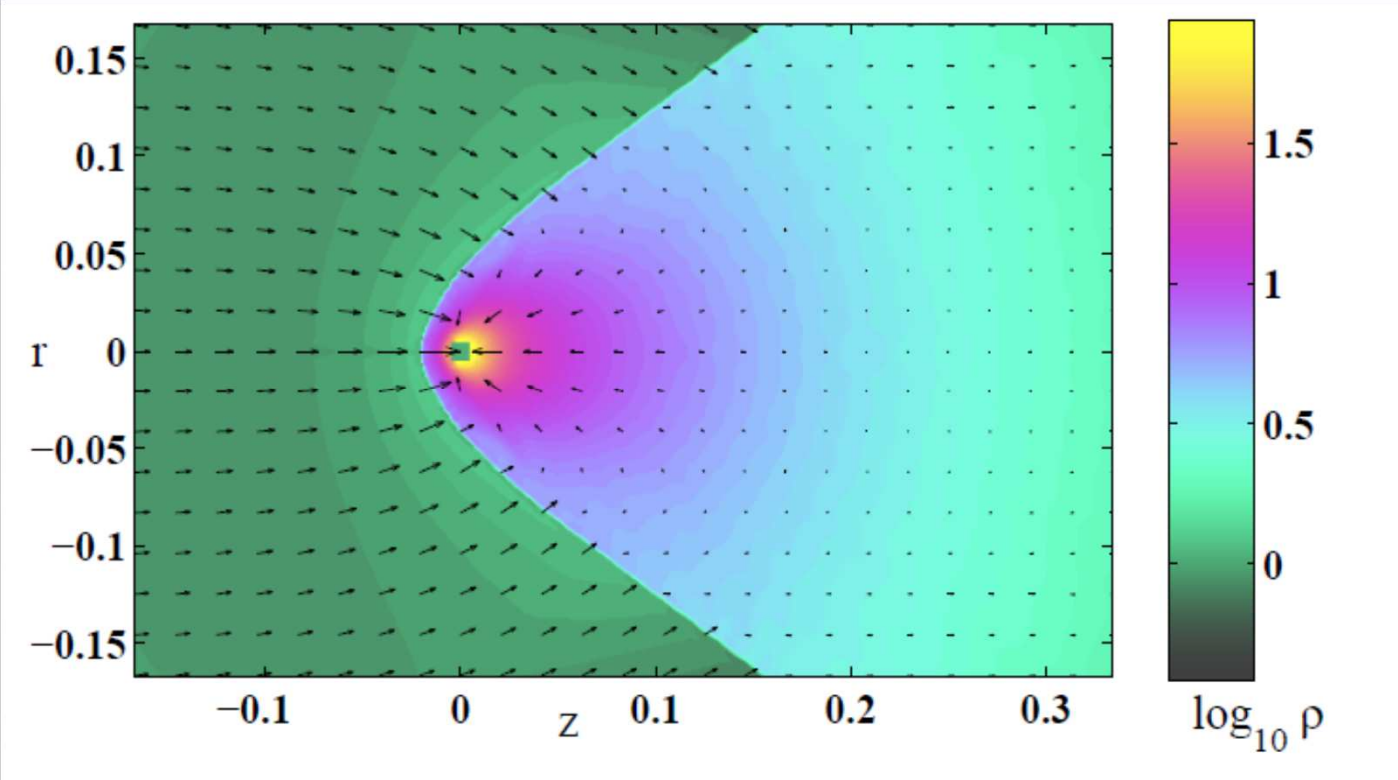

Traditional HD test: BHL accretion for $M = 3$. Central region for $t = 7.0\ t_0$ is shown, where t_0 – is crossing time (ΔZ / v∞). The background represents logarithm of density. The length of the arrows is proportional to the poloidal velocity. Matter accumulates around NS and accretes onto its surface. Typical BHL accretion.

II. MHD Simulation of Accretion

Hydrodynamic case

$\dot{M} / \dot{M}_{BHL}$

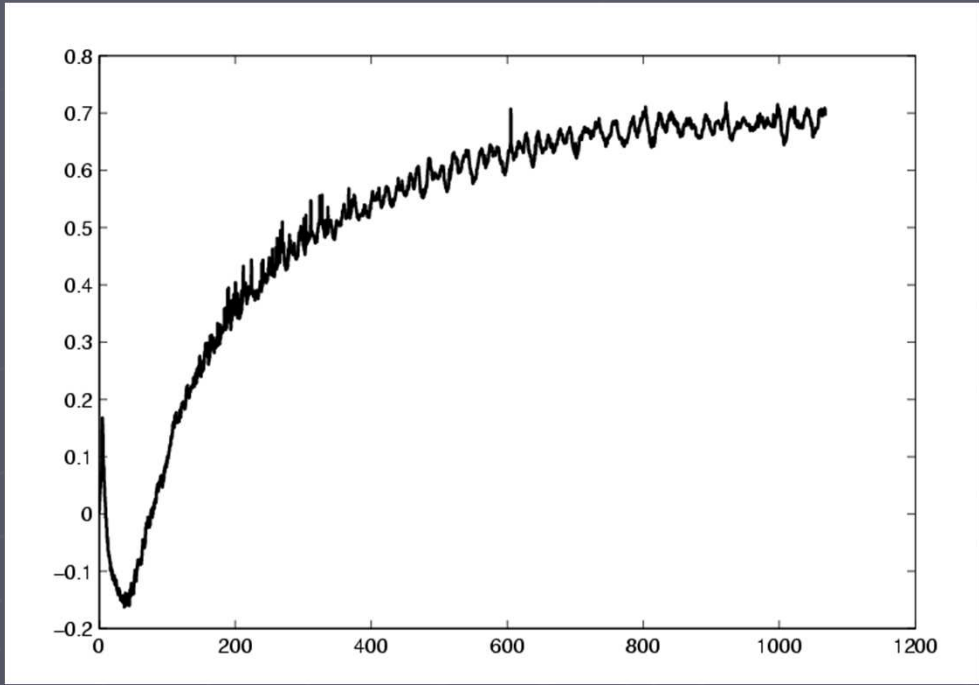

t

An accretion rate corresponds to analytical one with correction to α - parameter

$$\dot{M}_{\rm BHL} = \frac{4\pi\alpha (G M_*)^2 \rho}{(v^2 + c_s^2)^{3/2}} \approx 7.4 \times 10^8 \frac{n}{v_{100}^3} M^2 \ \frac{\rm g}{\rm s} \ .$$

III. Slow Rotating and Moving NS

$R_A < R_{acc}$

Gravitational focusing is important.

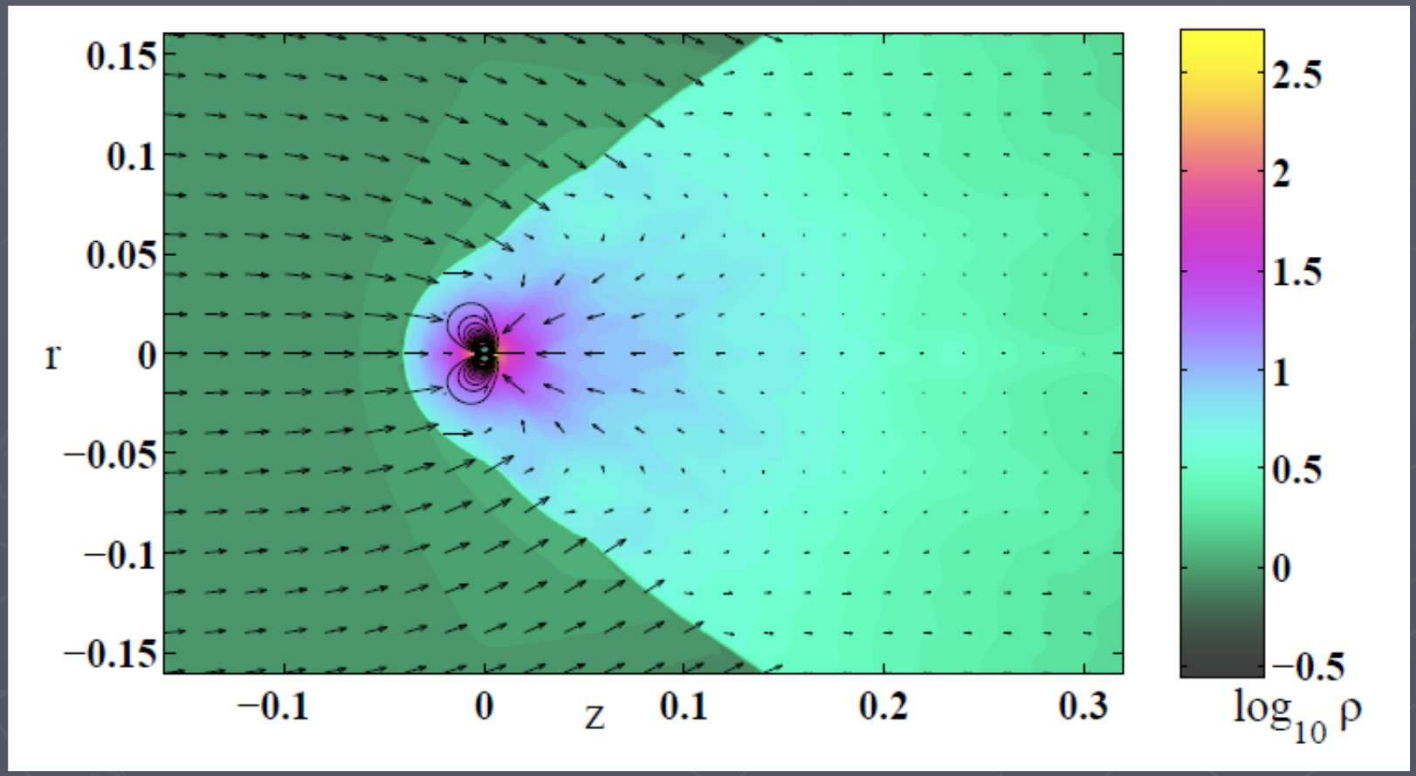

Matter flow around a weakly magnetized star moving through the ISM medium with Mach number $M = 3$ at time $t = 4.5\ t_0$. The background is logarithm of density. The length of the arrows ~ poloidal velocity. Magnetic field acts as an obstacle for the flow. Matter forms a shock wave, accumulates around NS and accretes onto its surface.

III. Slow Rotating and Moving NS

$R_A < R_{acc}$

Gravitational focusing is important.

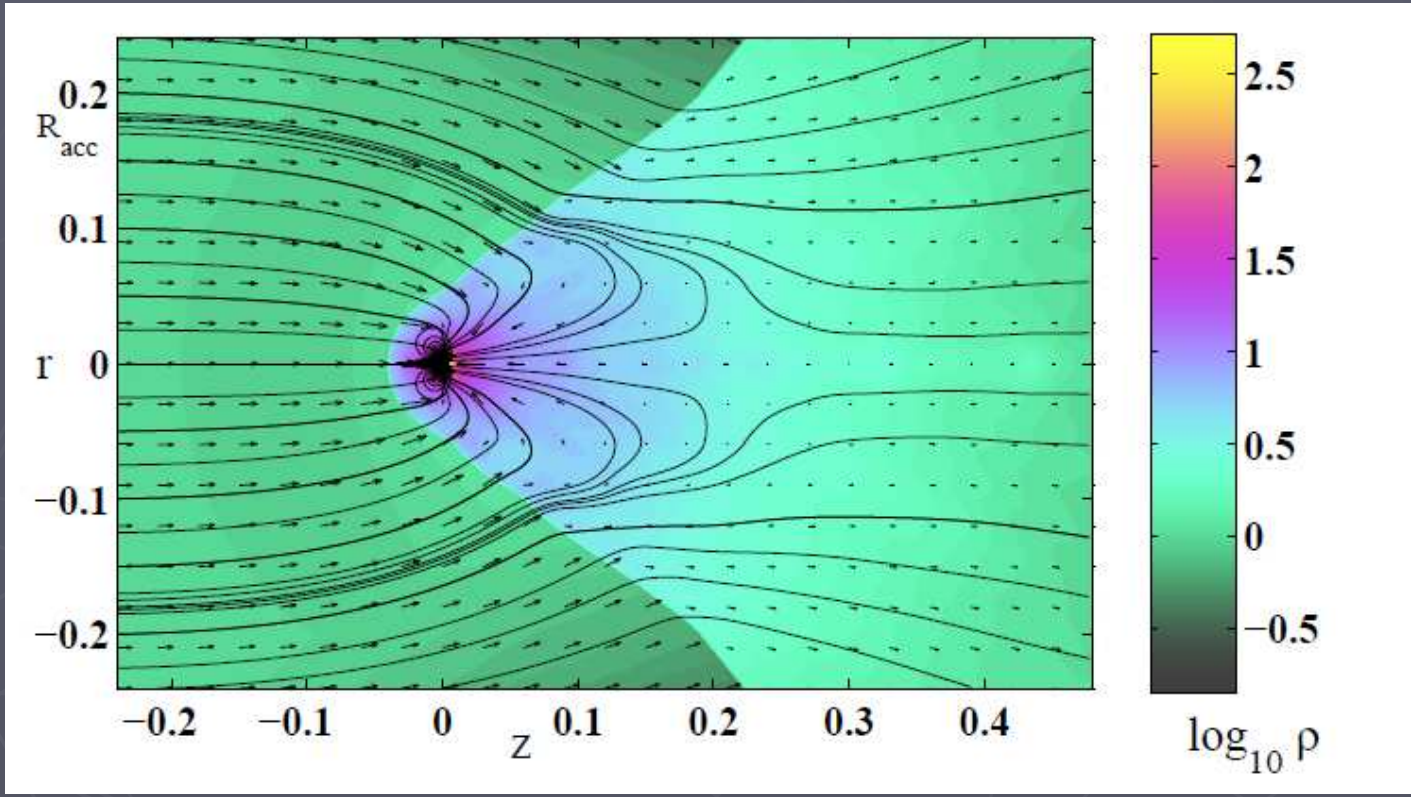

Matter flow around a weakly magnetized star moving through the ISM with Mach number $M = 3$ at a late time $t = 4.5\ t_0$. The background = the logarithm of density and the solid lines are streamlines. The length of the arrows ~ poloidal velocity. Matter inside Racc accretes onto NS, matter outside Racc flies away.

III. Slow Rotating and Moving NS

$R_A < R_{acc}$

Gravitational focusing is important.

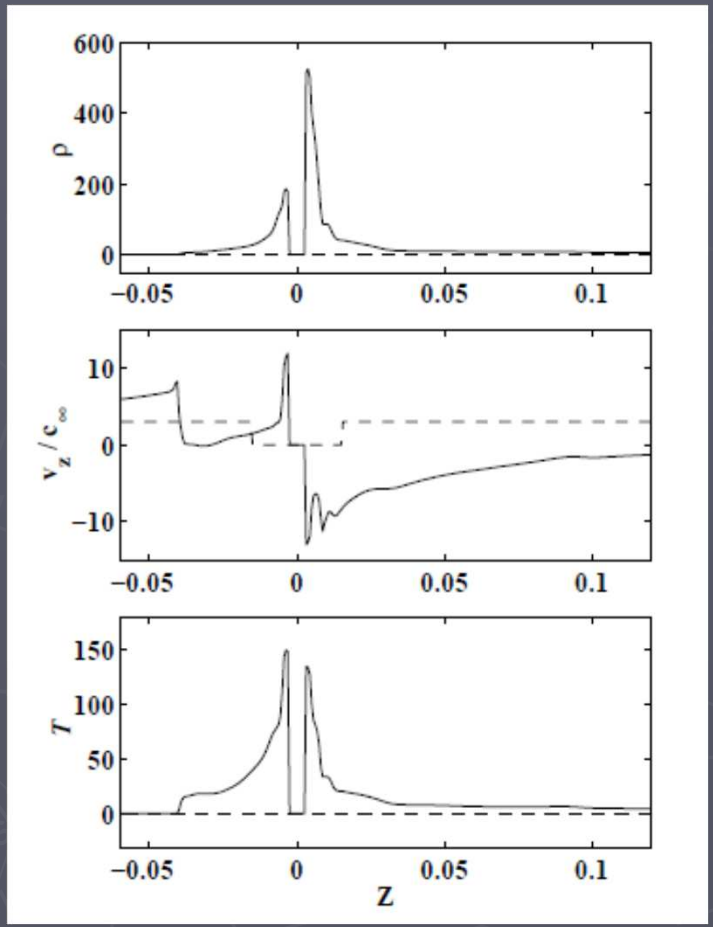

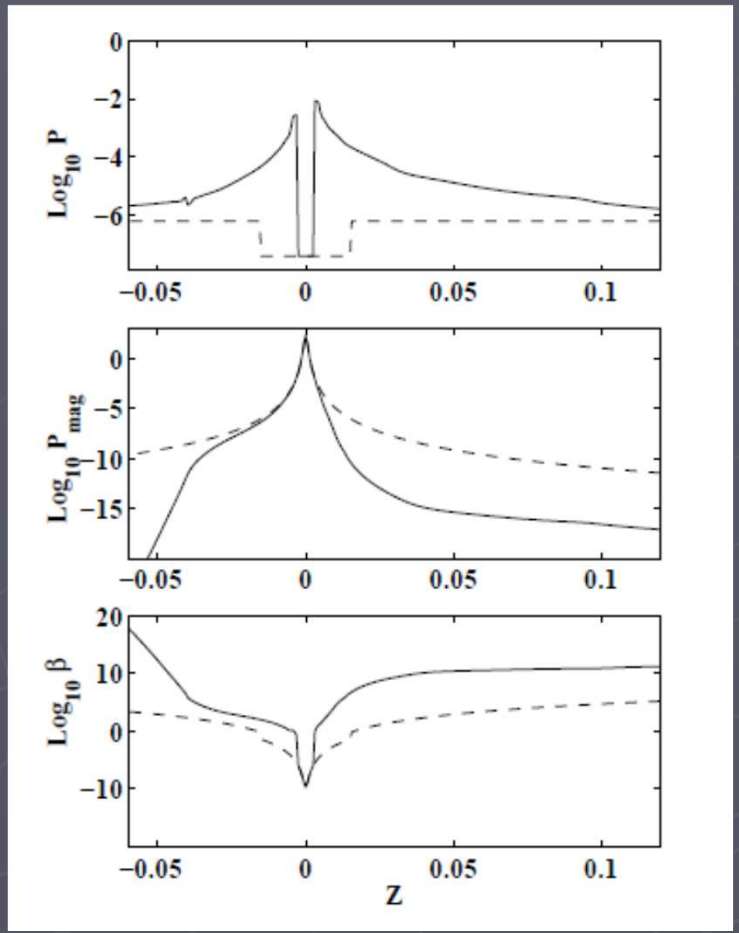

Dashed line is = initial distribution

III. Slow Rotating and Moving NS

$R_A < R_{acc}$

Gravitational focusing is important.

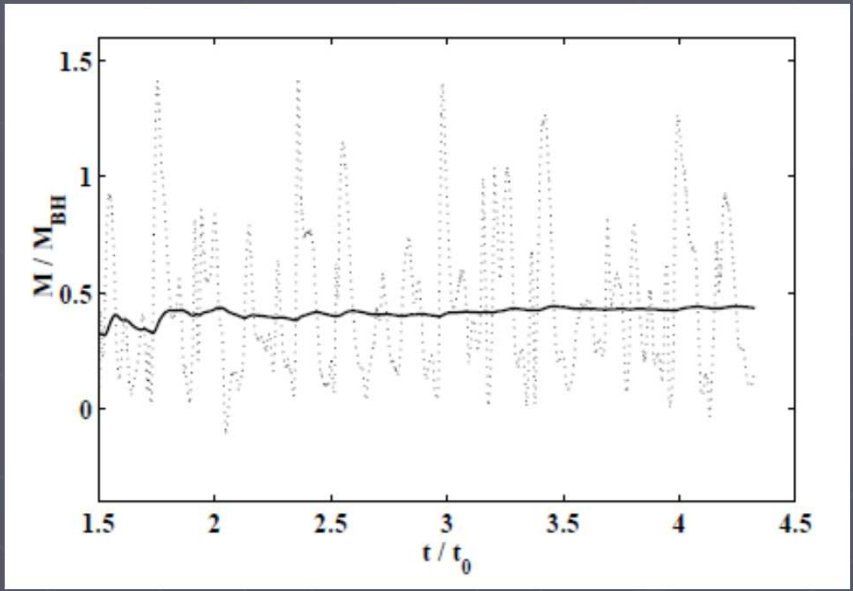

Dependence of mass accretion rate on time. The dashed lines give the mass accretion rate normalized in Bondi-Hoyle rate, while the solid lines give the integrated mass flux. Time is measured in the crossing time units, $\Delta Z / v\infty$.

III. Slow Rotating and Moving NS

$R_A < R_{acc}$

Oscillations

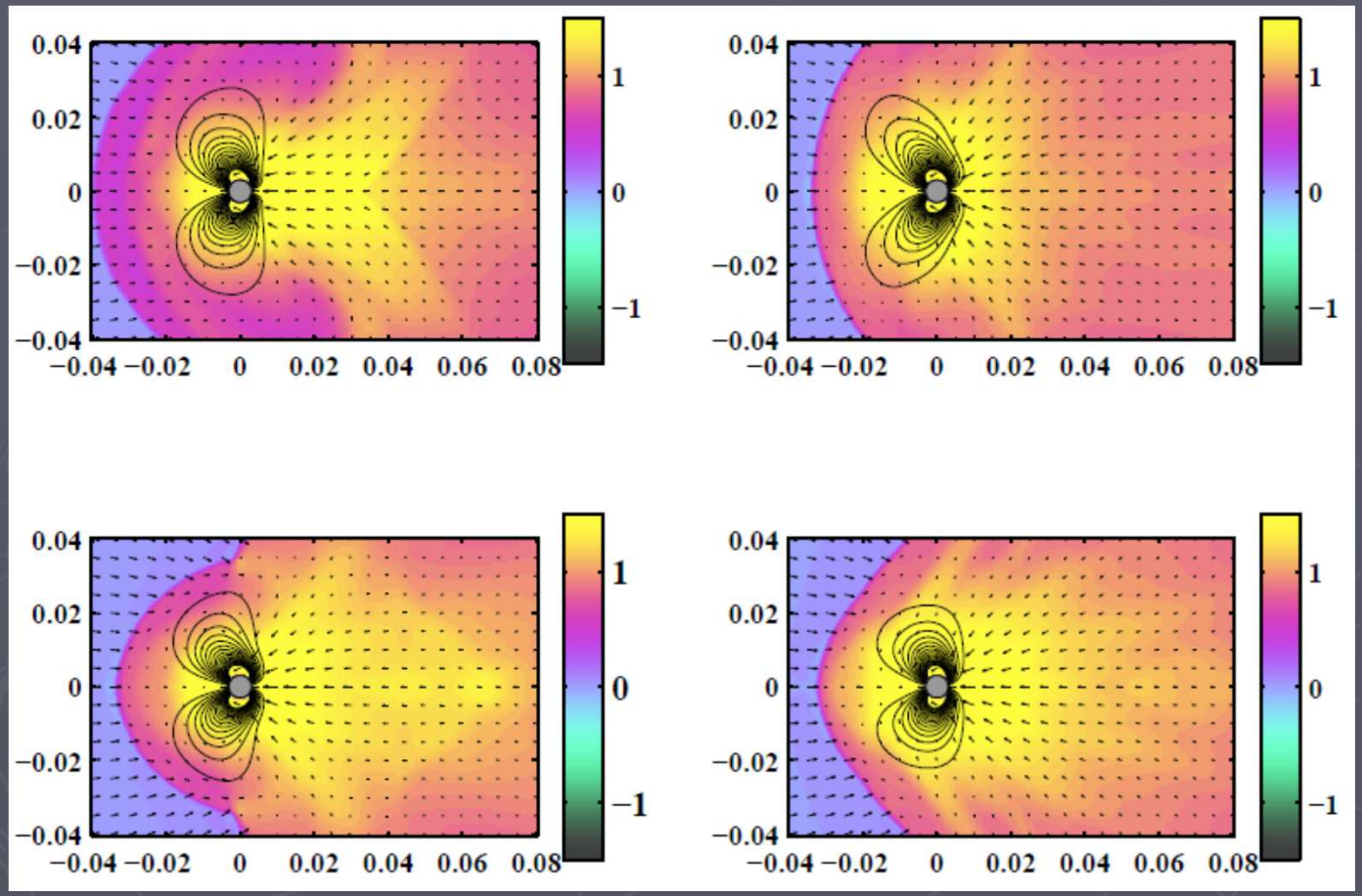

Accretion flow for different moments: = 0.7 t0, t = 1.4 t0, t = 2.0 t0 and t = 2.7 t0. Time is measured in the crossing time units, $\Delta Z / v\infty$.

III. Slow Rotating and Moving NS

$R_A \sim R_{acc}$

Gravitational focusing is less important.

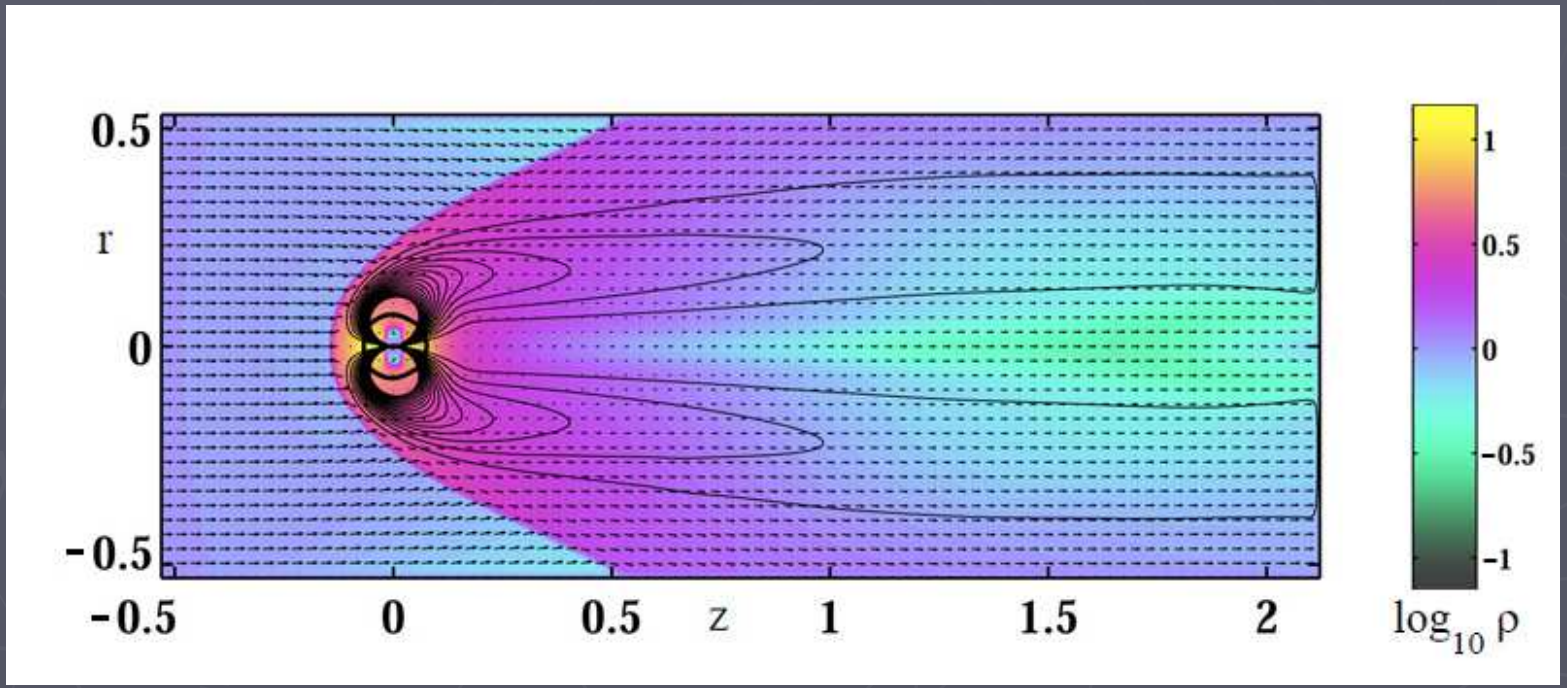

Results of simulations of accretion to a magnetized star at Mach number **M = 3**. Poloidal magnetic B field lines and velocity vectors are shown. Magnetic field acts as an obstacle for the flow; and clear conical shock wave forms. Magnetic field line are stretched by the flow and forms a magnetotail.

III. Slow Rotating and Moving NS

$R_A \sim R_{acc}$

Gravitational focusing is less important.

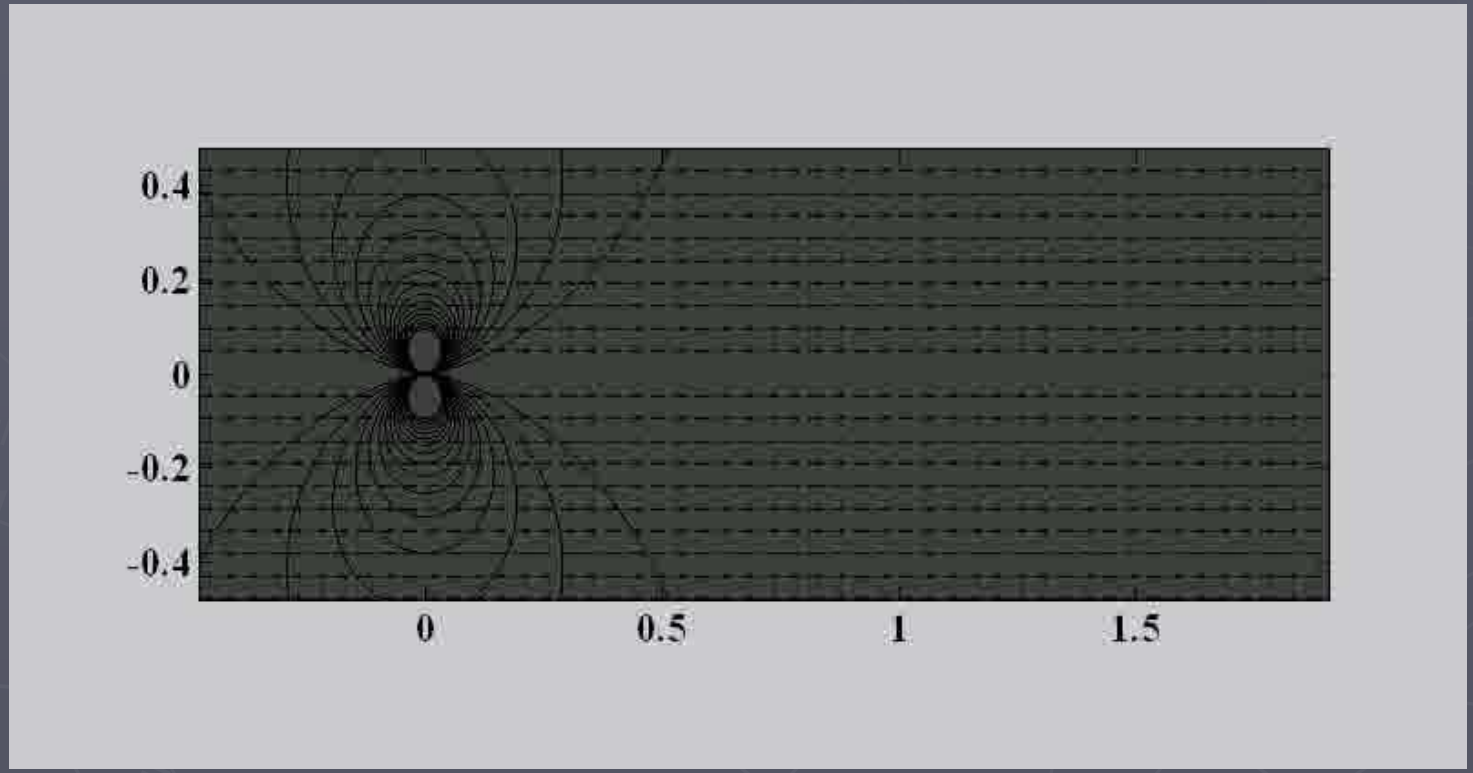

Results of simulations of accretion to a magnetized star at Mach number **M = 3**. Poloidal magnetic B field lines and velocity vectors are shown. Magnetic field acts as an obstacle for the flow; and clear conical shock wave forms. Magnetic field line are stretched by the flow and forms a magnetotail.

III. Slow Rotating and Moving NS

$R_A \sim R_{acc}$

Gravitational focusing is less important.

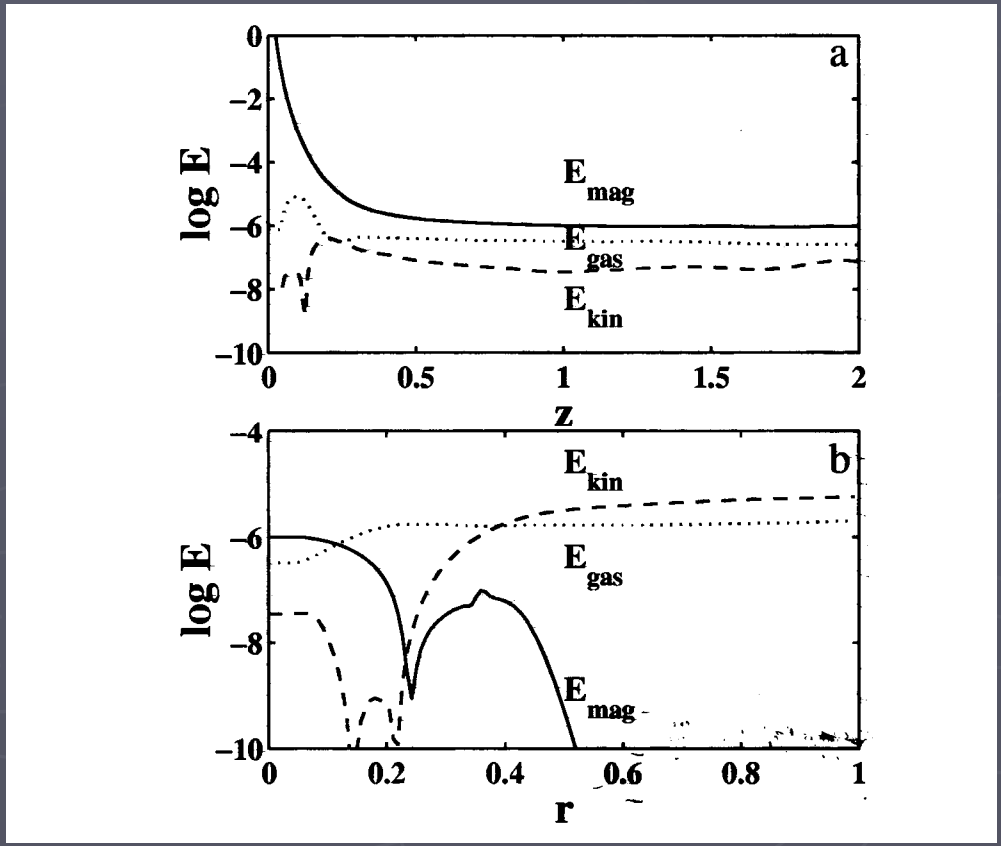

Energy distribution in magnetotail. M=3, magnetic energy dominates.

III. Slow Rotating and Moving NS

$R_A > R_{acc}$

Gravitational focusing is not important.

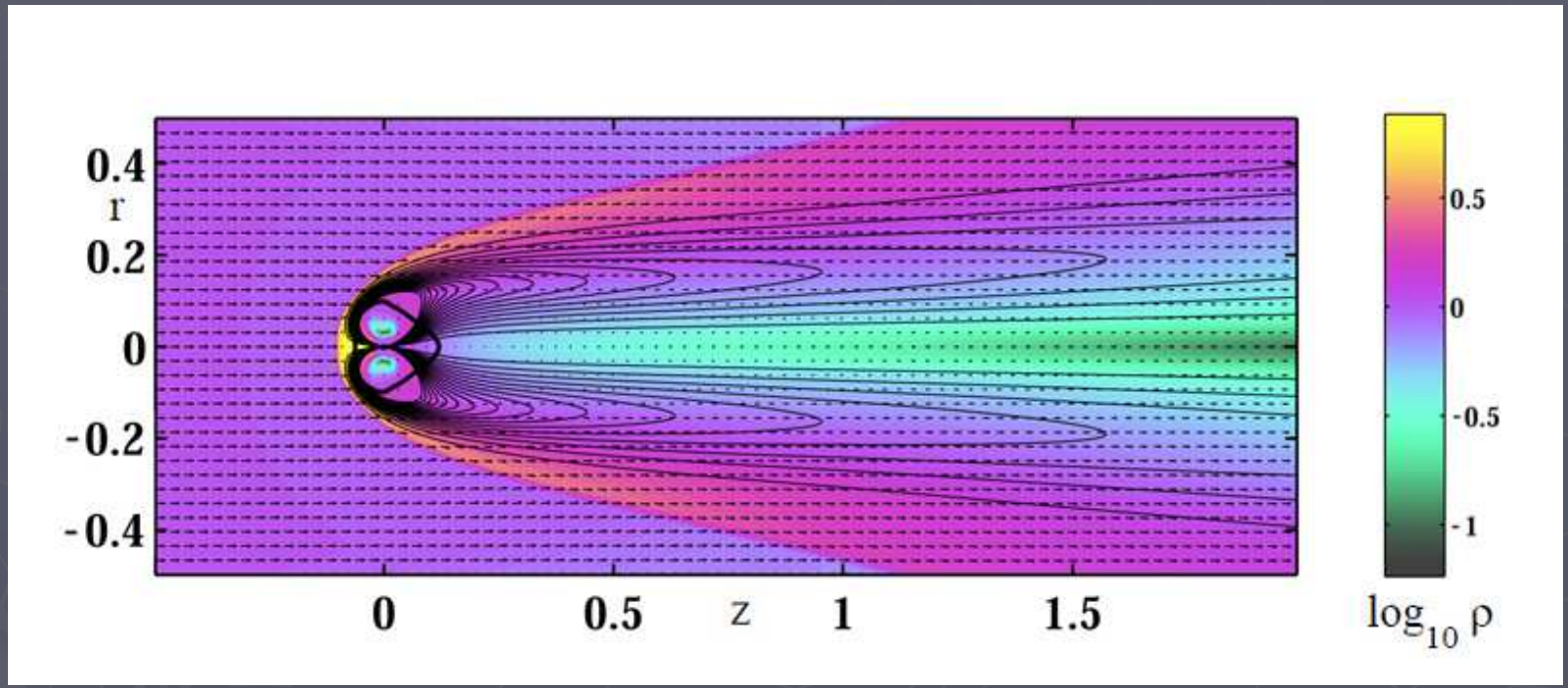

Results of simulations of accretion to a magnetized star at Mach number **M = 6**. Poloidal magnetic B field lines and velocity vectors are shown. Bow shock is narrow. Magnetic field line are stretched by the flow and forms long magnetotail. Accretion onto NS is impossible.

III. Slow Rotating and Moving NS

$R_A > R_{acc}$

Gravitational focusing is not important.

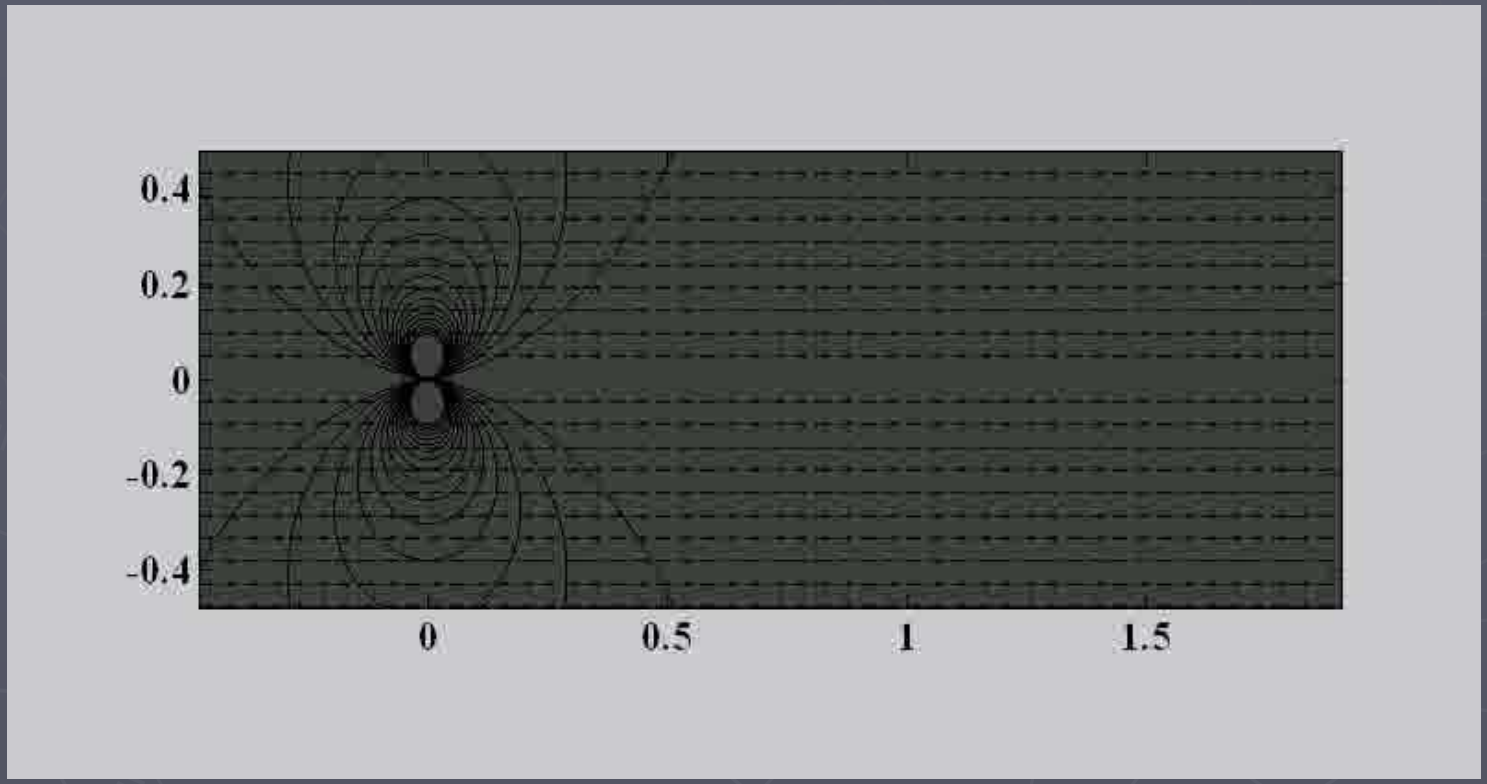

Results of simulations of accretion to a magnetized star at Mach number **M = 6**. Poloidal magnetic B field lines and velocity vectors are shown. Magnetic field line are stretched by the flow and forms long magnetotail.

III. Slow Rotating, Fast Moving NS

$R_A >> R_{acc}$

Gravitational focusing is not important.

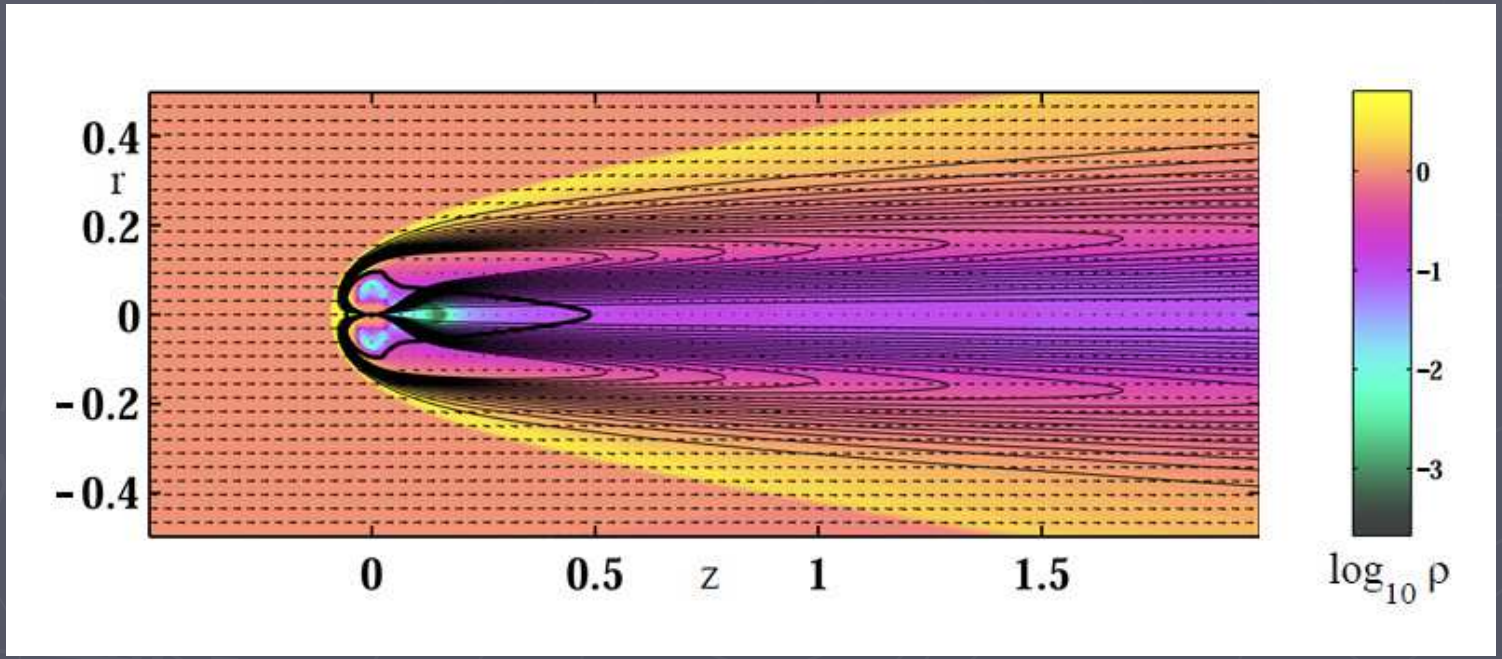

Georotator regime. Results of simulations of accretion to a magnetized star at Mach number **M = 10**. Poloidal magnetic B field lines and velocity vectors are shown. Bow shock is narrow. Magnetic field line are stretched by the flow and forms long magnetotail. t = 4.5 t_0 Density in the magnetotail is low.

III. Slow Rotating, Fast Moving NS

$R_A >> R_{acc}$

Gravitational focusing is not important.

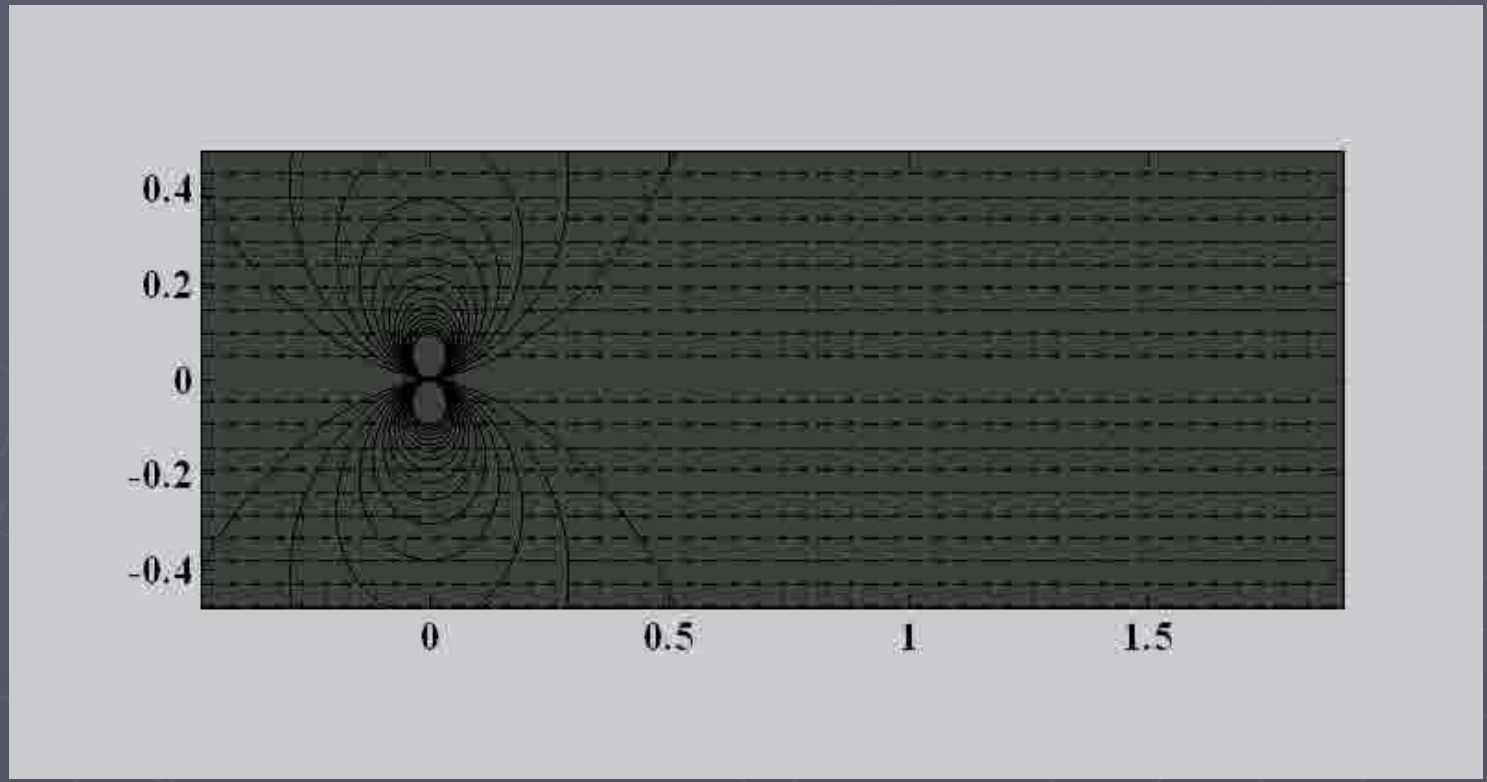

Georotator regime. Results of simulations of accretion to a magnetized star at Mach number **M = 10**. Poloidal magnetic B field lines and velocity vectors are shown. Magnetic field line are stretched by the flow and forms long magnetotail.

III. Slow Rotating, Fast Moving NS

$R_A >> R_{acc}$

Density and field variation at different Mach numbers.

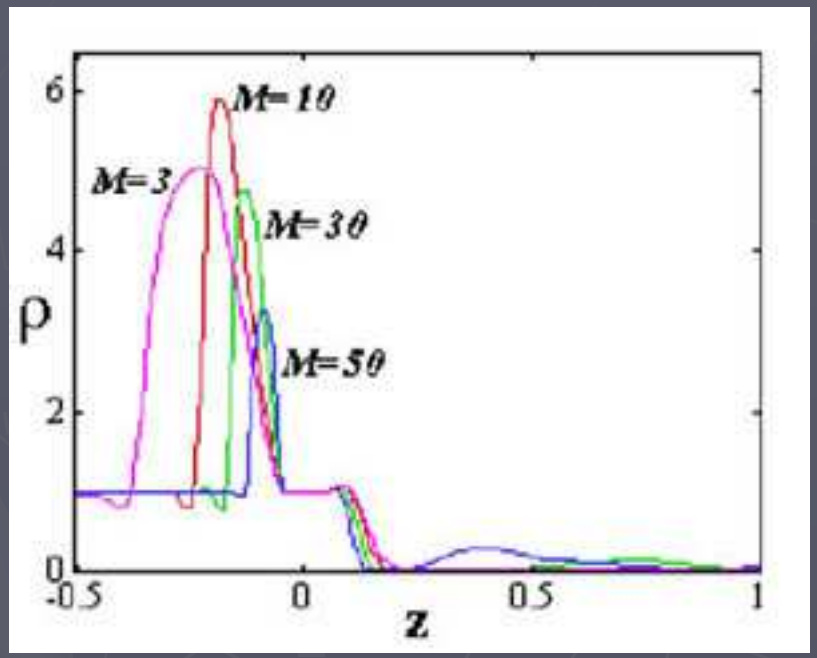

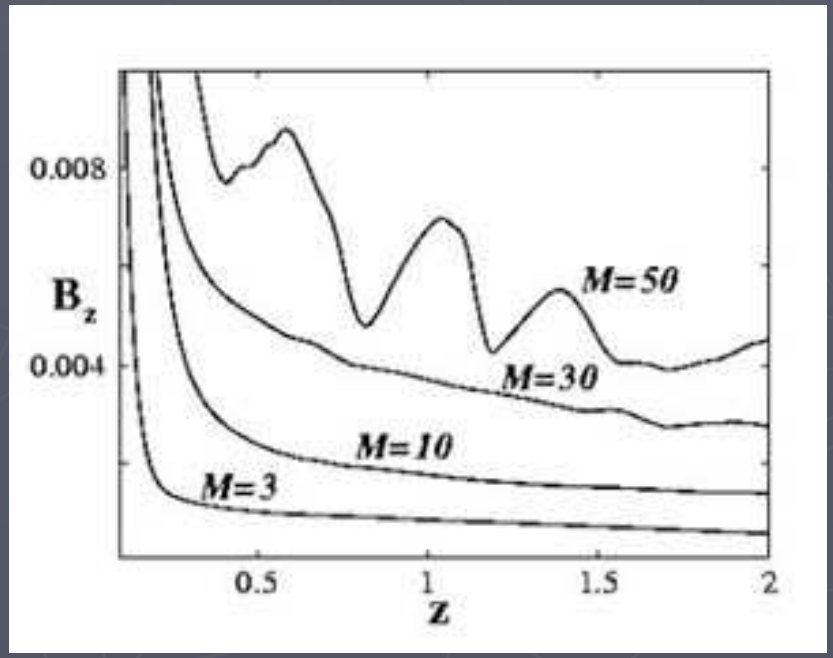

Density in the magnetotail is low. Magnetic field in the magnetotail reduced gradually.

IV. Fast Rotating and Moving NS

$R_A > R_{acc}$

Example of matter flow for a star rotating at $\Omega_* = 0.7\ \Omega_K$ and M=3.

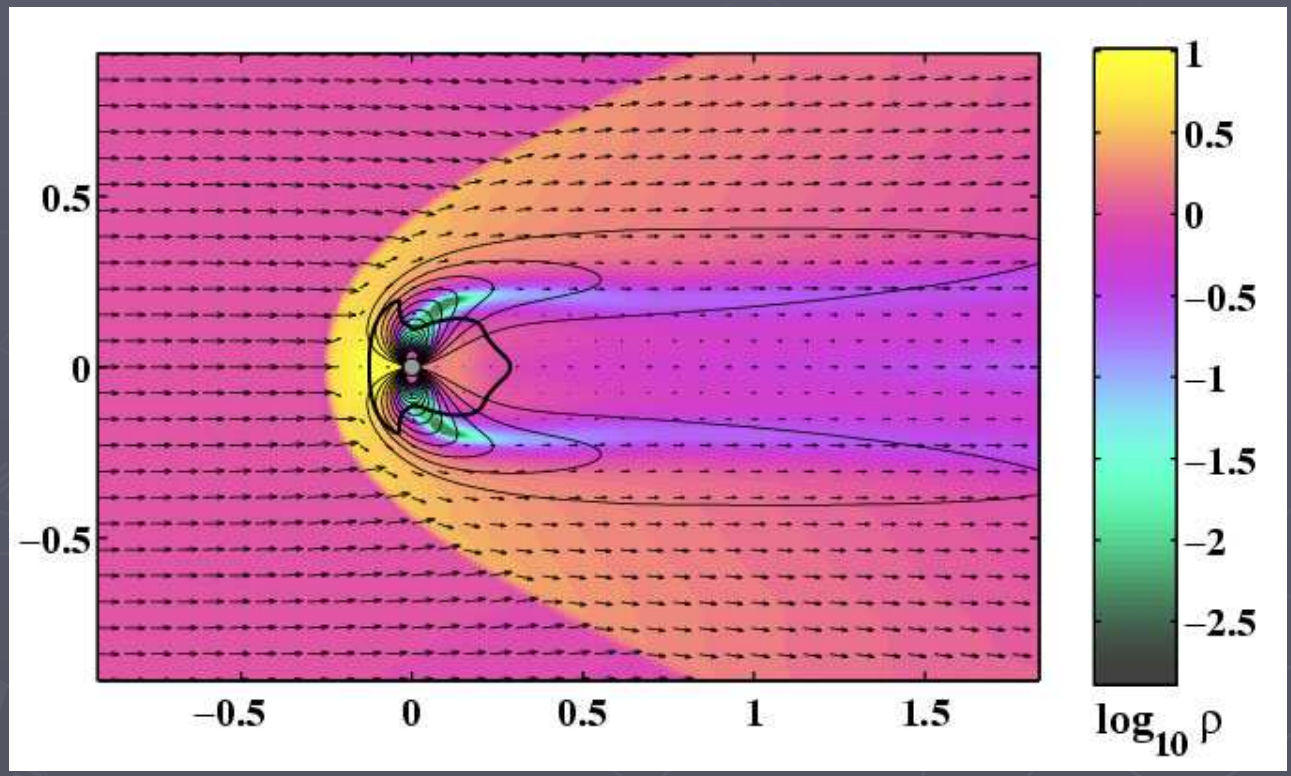

The magnetic field of the star acts as an obstacle for the flow and a conical shock wave forms. At larger distances the field is stretched by the flow, forming long magnetotail. The rapidly rotating magnetosphere expels matter outward in the equatorial region. This matter first flows radially outward, then along Z-direction.

IV. Fast Rotating and Moving NS

$R_A > R_{acc}$

Example of matter flow for a star rotating at $\Omega_* = 0.7\ \Omega_K$ and $M=3$.

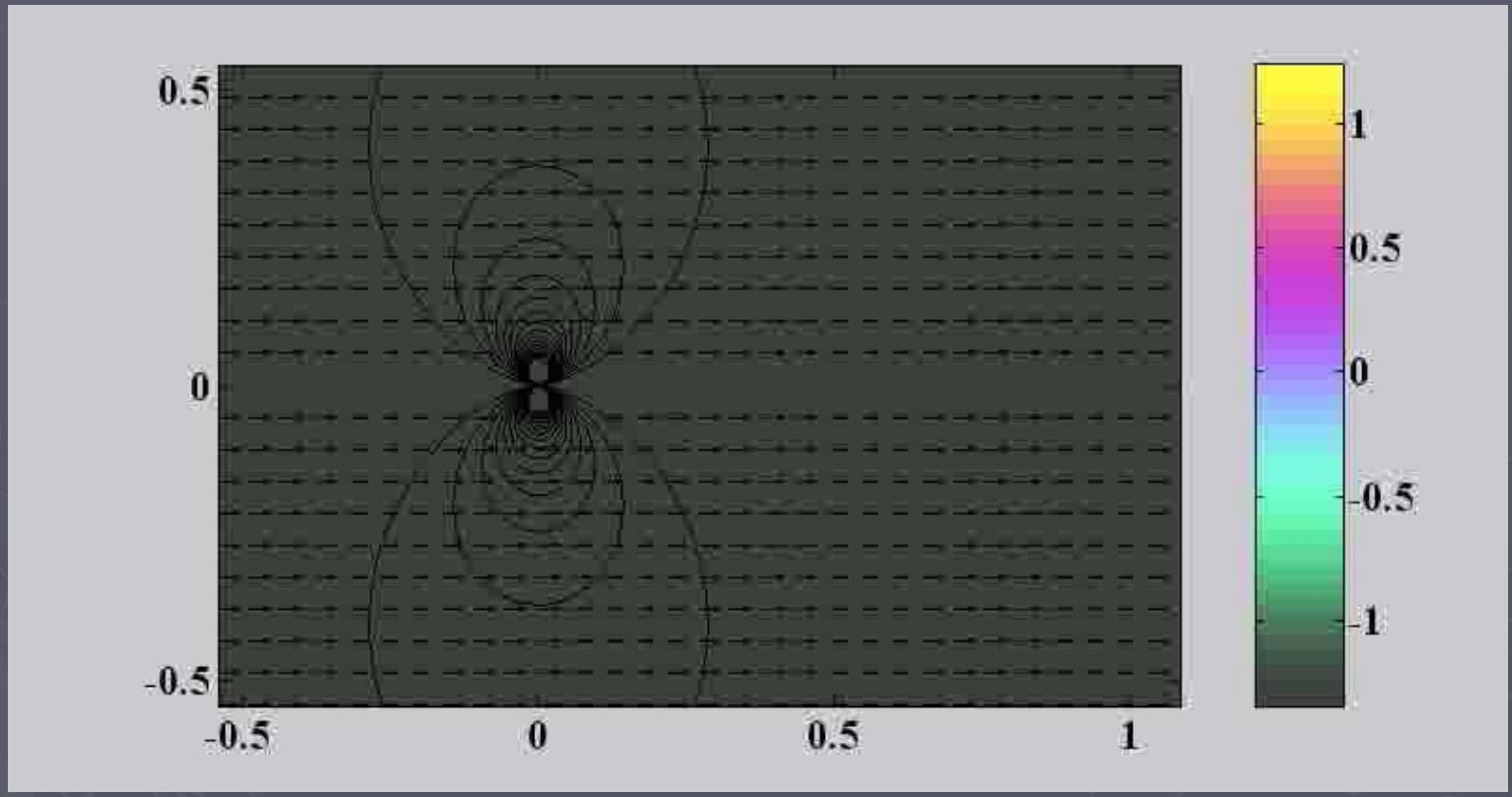

The magnetic field of the star acts as an obstacle for the flow and a conical shock wave forms. At larger distances the field is stretched by the flow, forming long magnetotail. The rapidly rotating magnetosphere expels matter outward in the equatorial region. This matter first flows radially outward, then along Z-direction.

IV. Fast Rotating and Moving NS

$R_A > R_{acc}$

An angular momentum flux

Rapidly rotating star looses an angular momentum and spins down. We can estimate the total angular momentum loss rate from the star by evaluating the integral over the surface around the star's magnetosphere.

$$\dot{L} = -\int d\mathbf{S} \cdot \left(\rho \mathbf{v}_p r v_\phi - \frac{\mathbf{B}_p r B_\phi}{4\pi} \right)$$

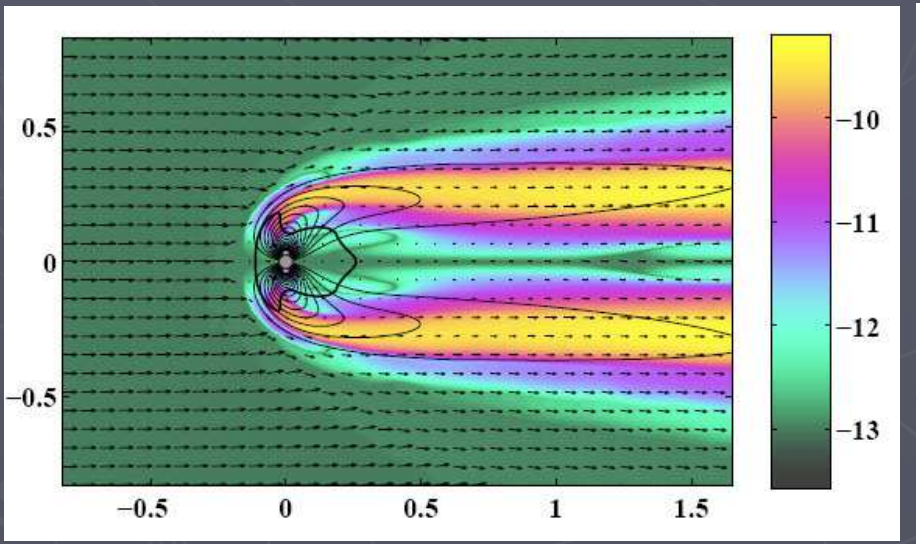

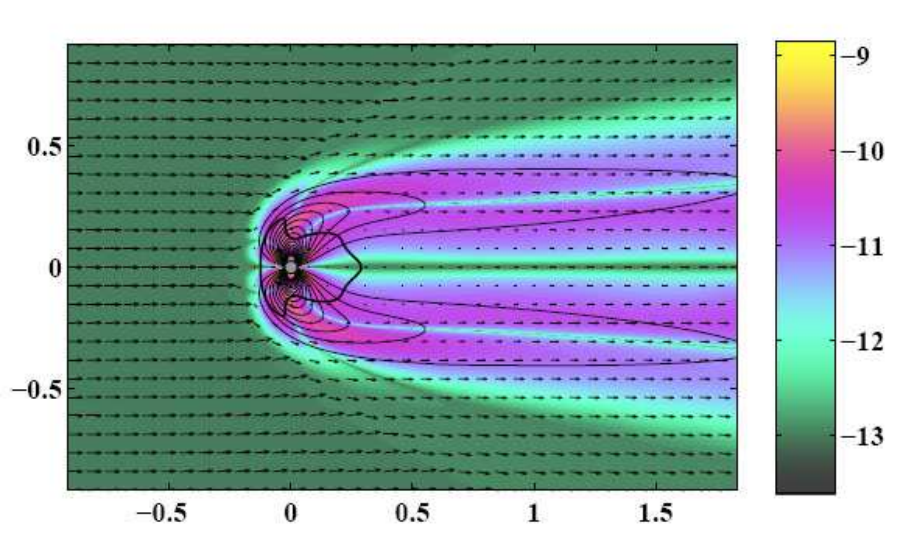

Left panel: Angular momentum flow connected with matter.
Right panel: Angular momentum flow connected with magnetic field.

IV. Fast Rotating and Moving NS

$R_A > R_{acc}$

An angular momentum evolution

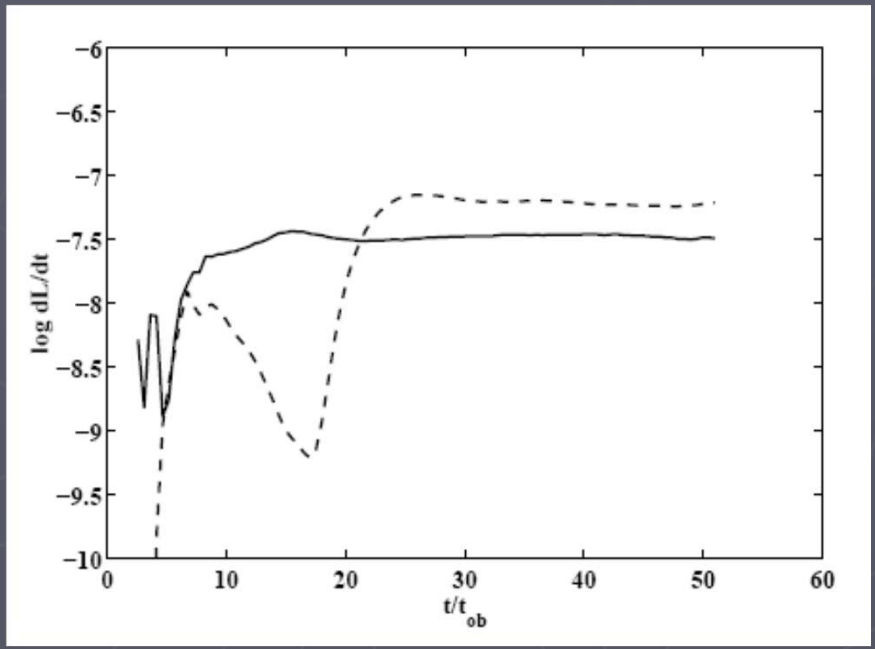

The total angular momentum flux around the magnetosphere (solid line) becomes constant approximately after 10-15 rotation periods of the star. As the matter is passing the angular momentum flux in tail (dotted line) is increasing up to value of flux around the magnetosphere and becomes constant. Figure shows that total flux across section z=0.6 becomes constant and equal to flux around the magnetosphere approximately after 26 rotation periods.

IV. Fast Rotating and Moving NS

$R_A > R_{acc}$

Dependence of the angular momentum loss rate on parameters

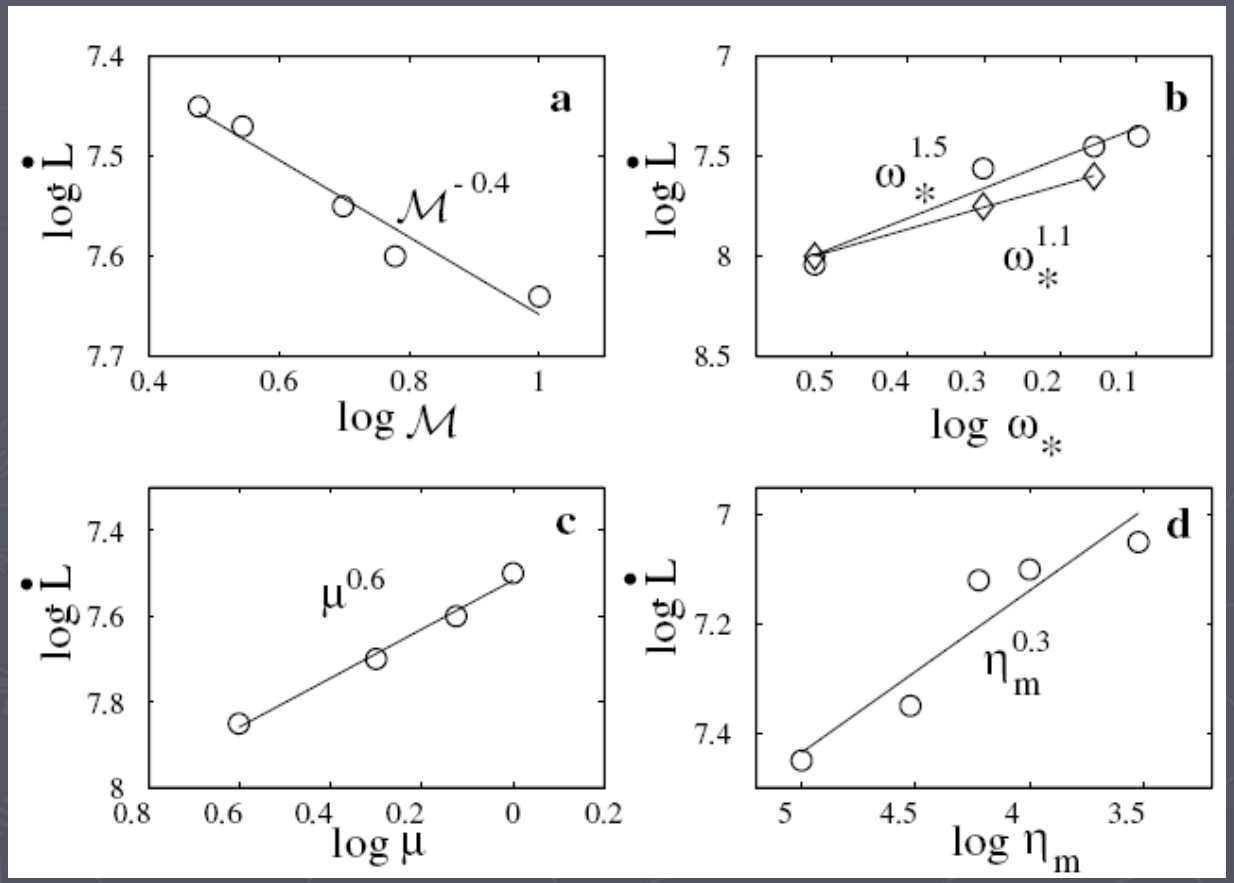

IV. Fast Rotating and Moving NS

$R_A > R_{acc}$

The summary of scaling laws

$$\frac{dL}{dt} \propto -\eta^{0.3}\mu^{0.6}\rho^{0.8}\mathcal{M}^{-0.4}\Omega_*^{1.5}$$

The characteristic time of spin-down of magnetar is

$$T = L_*/|\dot{L}| \approx 10^4\ n_1^{-1} c_{30}^4 B_{15}^{-0.6} P_5^{0.5} \mathcal{M}_3^{0.4}\ \mathrm{yr}\ .$$

For periods $P_* \sim 10^3$ s, which correspond to beginning of the propeller stage, the evolution scale will be $\Delta T = 10^3$ years, while at period $P_* \sim 10^6$ s corresponding to the end of propeller stage $\Delta T = 3 \times 10^4$ years. Thus we see that magnetars are expected to spin down very fast at the propeller stage

V. Observations

VLT observations by Kerkwijk and Kulkarni

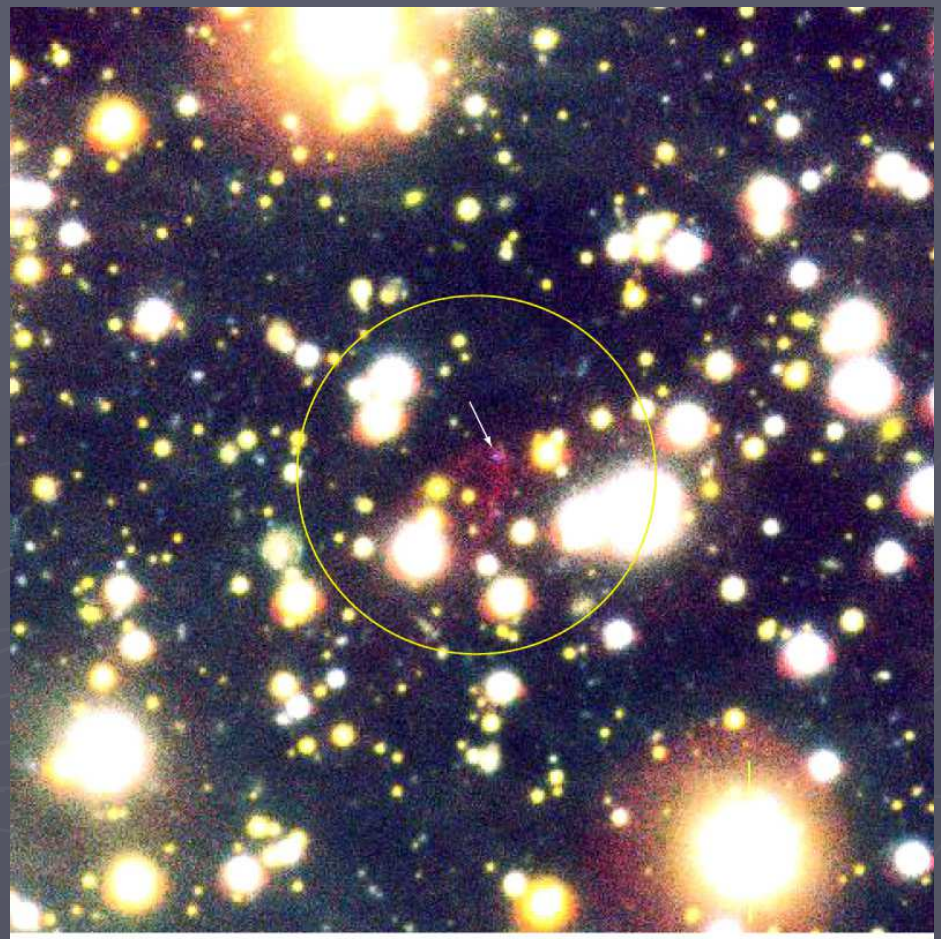

A Bowshock Nebula Near the Neutron Star RX J1856.5-3754 (Detail)
(VLT KUEYEN + FORS2)

ESO PR Photo 23b/00 (11 September 2000)

V. Observations

Observations of pulsar tails

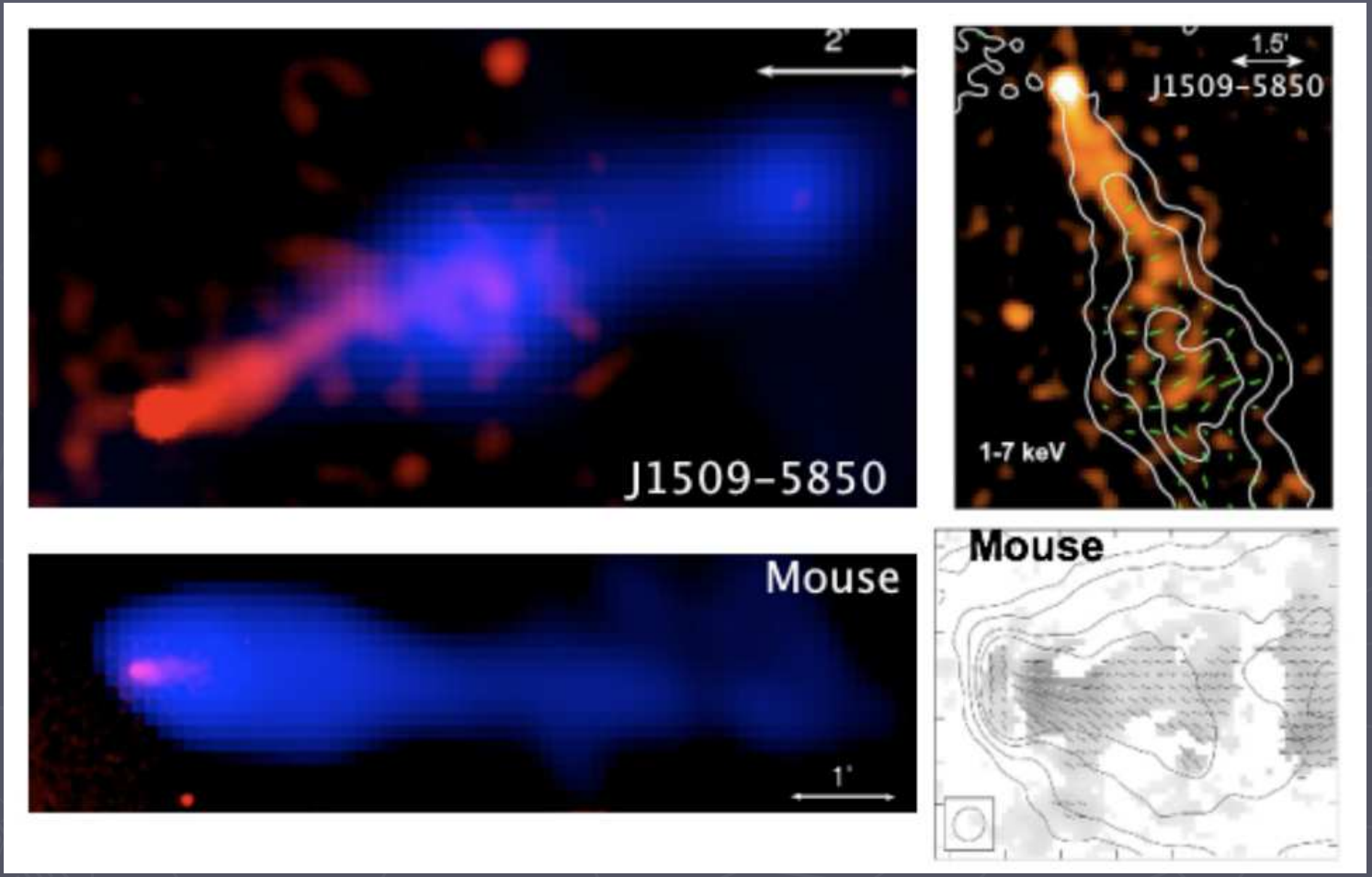

X-ray and radio images of the very long pulsar tails (PSR J1509-5850 - top; Mouse - bottom panels)